Jha and Puppala *Geotherm Energy (2017) 5:3*
DOI 10.1186/s40517-017-0061-4

Geothermal Energy

RESEARCH
Open Access

Assessment of subsurface temperature distribution from the gauged wells of Puga Valley, Ladakh

Shibani K. Jha* and Harish Puppala

*Correspondence: shibani@pilani.bits-pilani.ac.in
Department of Civil Engineering, Birla Institute of Technology and Science, Pilani, Rajasthan 333031, India

Abstract

Among the distinguished zones of geothermal potential in India, the Puga Valley is identified as one of the potential sites for tapping geothermal energy at industrial scale. The hydrogeological properties and the temperature variations with depth have been examined under the Geological Society of India by drilling borewells at a few locations. The temperature distribution is one of the most essential parameters in quantifying the energy potential of a geothermal reservoir in its life time. Such temperature distribution has not been mapped for the Puga Valley. 2D Kriging technique is adopted in this study to assess temperature distribution for thermal manifestation zone at various depths and these are further used to estimate the thermal gradients at ungauged locations of the valley. From the results obtained, it is observed that the thermal gradient in the eastern zone of the valley is relatively higher. This indicates a possible bottom heat source in the eastern zone of the valley. The results of this study could be helpful in identifying the distinctive conceivable locations of injection and production wells for the extraction of entrapped heat within the rock strata. Also, a priority order is drawn in terms of thermal gradients at gauged and ungauged locations which may be helpful in deciding the zones of high and low heat sources in the reservoir.

Keywords: Thermal gradient, Kriging, Thermal manifestation zone, Gauged wells, Ungauged wells, PGW (Puga geothermal well)

Background

After decades of research carried out in India by several government organizations, a decision has been taken to generate 1000 MW of electricity using geothermal energy by 2022. Geothermal energy is perceived as a hidden potential in the earth's crust. The USA, Indonesia, Philippines, Italy, Mexico and Iceland are the leading nations in utilizing this potential. Research efforts in India on geothermal energy date back to year of 1862 (Guha 1986). As a part of this effort, the Geological Survey of India explored 340 hot springs and a few potential geothermal provinces with an overall potential of 10,600 MW. These springs are grouped into seven geothermal provinces namely Himalayan (Puga–Chumathang), Sahara Valley, Cambay Basin, Son-Narmada-Tapi Lineament Belt, West Coast, Godavari Basin and Mahanadi Basin. However, subsequent research in exploring and tapping this energy resource remains inadequate and no remarkable progress has been achieved in the production of electricity on an industrial scale

(Chandrasekharam and Chandrasekhar 2015). One of the best locations among these identified geothermal zones is the Puga Hot Springs area. It is located at the junction of the Indian and Tibetan plates along the Indus Suture Zone. It lies in the southeastern part of Ladakh in Jammu and Kashmir and frames a part of the Himalayan geothermal belt, with geographical co-ordinates of 33°13′ to North and 78°19′ to East. This zone is identified as the highest potential zone with discharges concentrated in an east–west elongated area of 4 km^2, near the mouth of the Puga Valley (Craig et al. 2013). This zone, located in the eastern Ladakh region of Jammu and Kashmir, shows evidence of vigorous geothermal activity in the form of hot springs, mud pools, sulphur and borax deposits (Azeez and Harinarayana 2007).

The Indian government formed a committee in 1967 to investigate the possibility of geothermal exploration in India. After a few investigations, the committee submitted a detailed report of hot springs and potential geothermal provinces in 1983. This report is termed as the Hot Spring Committee report. This report mentioned various investigations in this zone (Azeez and Harinarayana 2007). Also, various other geo-scientific investigations followed consisting of geological, geochemical and shallow geophysical studies, which altogether highlight the significance of this region (Azeez and Harinarayana 2007). However, the lack of detailed deep reservoir information impairs further evaluation of the energy potential in geothermal Puga Valley.

The potential of a geothermal reservoir during its lifetime depends on the reservoir temperature, production flow rate, fluid properties, and injection and extraction temperature. The relation between these parameters can be mathematically expressed by Eq. 1 (Kruger 1995).

$$E = \int_{t_\mathrm{b}}^{t_\mathrm{a}} Q(t) \times \Delta h(T_I, T_E, t)\mathrm{d}t, \tag{1}$$

where E = Potential of the geothermal reservoir, Q = Production flow rate, t_a = Starting time of the reservoir, t_b = Application abandonment time, Δh = Difference in the enthalpy between the injected temperature and the extracted temperature, T_I = Injection temperature of the cold water, T_E = Extraction temperature of hot water.

In general, enthalpy is preferably used for simplified description of energy transfer term to represent system energy changes in many physical measurements at constant pressure. The magnitude of energy that can be drawn from a reservoir during its lifetime depends on the duration of plant operation which is reflected by "starting time of the reservoir" and "application abandonment time". Furthermore, enthalpy associated with the extracted fluid is a function of injection and extraction temperature which is a time-dependent variable. The provided equation is the generalized form of the energy equation. From Eq. 1, it is explicable that the output from a geothermal reservoir depends on the difference in the enthalpy, which in turn directly depends on the reservoir temperature distribution. This can be mathematically expressed by Eq. 2

$$E \propto (Q, T_\mathrm{s}), \tag{2}$$

where, T_S = Subsurface or reservoir temperature, Q = Production flow rate.

Geothermal gradient is a spatially varying geophysical parameter. Thus, the mapping of temperature at different depths helps in predicting the spatial variation of geothermal gradient in the valley. Thus, the present study focuses on developing steady state or equilibrium temperature distribution of the reservoir. Transient temperature distribution arises under non-equilibrium conditions like injection and extraction. Such studies are to be performed by coupled fluid flow and energy transport simulations. The equilibrium state of the reservoir provides the initial condition of the reservoir for transient simulation studies, and it also helps in selecting proper injection and production well locations forming doublets during the extraction of the entrapped heat from a particular stratum of a geothermal reservoir. In case of the Puga Valley reservoir, temperature vs. depth data are available only at a few gauged locations which were also restricted to limited shallow depths. Since temperature distribution is an important prerequisite to study the geothermal potential of any reservoir, an emphasis has been made in this study to map the temperature variation in the thermal manifestation zone at various depths. From existing literature, it is noted that Kriging is a suitable technique to determine the variation of geophysical parameters (Agemar et al. 2012; Rühaak 2014). Various Kriging interpolation techniques are generally used for the estimation of ungauged parameters in the field of geostatistics (Li 2008). These techniques have also been used in the fields of meteorology, water resources, marine and soil sciences, agriculture, and ecology (Li 2008). The Kriging technique is used to interpolate the concentrations of cobalt and copper in the top layer of soils and in the preparation of field extent soil property maps (Moyeed and Papritz 2002; Bishop and Mc Bratney 2001). It is also used in mapping the median grain-size distribution of the sand fraction at Belgian Continental Shelf (Verfaillie et al. 2006). In addition to these, it is noticed that ordinary Kriging and universal Kriging have been adopted in most of the studies including the estimation of subsurface temperature distribution (Chiles and Gable 1984; Bonte et al. 2010; Garibaldi et al. 2009; Agemar et al. 2012; Rühaak et al. 2014) and also for the interpolation of geostatistical parameters at unsampled locations.

The choice to use ordinary Kriging or universal Kriging depends on the type of existing data and the trend of data spread within it. If the trend follows simple functions, then universal Kriging is used; otherwise, ordinary Kriging is preferred to estimate a parameter at ungauged locations. It is observed that the temperature vs. depth data for gauged well locations disclose no common trend, which is discussed further in the subsequent sections. Therefore, ordinary Kriging interpolation technique was adopted in this study to map 2D temperature distribution in the thermal manifestation zone. The 2D temperature distributions are evaluated at every 10 m depth till 50 m. From the obtained 2D temperature distribution for thermal manifestation zone, thermal gradients for ungauged well locations are further estimated. In addition to this, average thermal gradients for all the gauged and ungauged locations are evaluated and a priority order in terms of highest to lowest thermal gradient is drawn. Such order may be helpful in identifying higher to lower heat source zone and prioritizing the locations for further deep exploration.

Geographical and hydrothermal information of Puga geothermal valley

The Puga Valley is located in the Ladakh district, which is 1600 km north of New Delhi. It is at an altitude of about 4400 m with an uneven terrain as shown in Fig. 1. It is found that the Puga Valley has more than one hundred hot springs with temperatures varying from 35 to 84 °C (boiling point of water at these altitudes) and it has a discharge of up to 5 L/s. This area exhibits extensive patches of warm ground, sulphur condensates, borax deposits, mud pools and hot water seepages (Gupta 2009). The hot springs emerge along a fault in Puga Nala of the valley. The Puga Valley, trending in an almost east–west direction, stretches over a length of about 15 km and a maximum width of about 1 km. It is a part of the central tectonic belt characterized by the volcanic sedimentary assemblages of rocks belonging to the Sumdo group and bounded by prominent faults (Harinarayana et al. 2006). These faults act as a conduit for transportation of the hot water from deeper levels. The valley is covered by the recent and sub-recent deposits such as glacial moraines, aeolian sand and scree. Furthermore, it is encrusted with borax, sulphur and other hot spring deposits. These unconsolidated sediments extend to the subsurface up to 15–65 m depth. Thereafter, the hard reconsolidated breccia lies and extends up to the depth of the basement. The basement rock consists of paragneisses and schists and is known as the Puga formation. This formation belongs to Palaeozoic age. The geology of this formation has been discussed by many researchers (Tewari 1964; Shanker et al. 1975, 1976, 1981).

After the commencement of the Hot Spring Committee by the government of India in 1967 (Geological Survey of India 1991), various geo-investigations, including exploratory drilling and studies on geothermal energy utilization on an experimental basis were carried out. These clusters are termed as diverse geothermal areas based on their occurrence in specific geo-tectonic, geological and structural settings. These regions include orogenic belt, structural grabens, deep fault zones and active volcanic regions etc. The generation of electricity at industrial scale from geothermal reservoir needs temperature distribution information till the greater depths and over continuous stretch. However, due to the technical difficulties, the number of borewell locations explored in the Puga

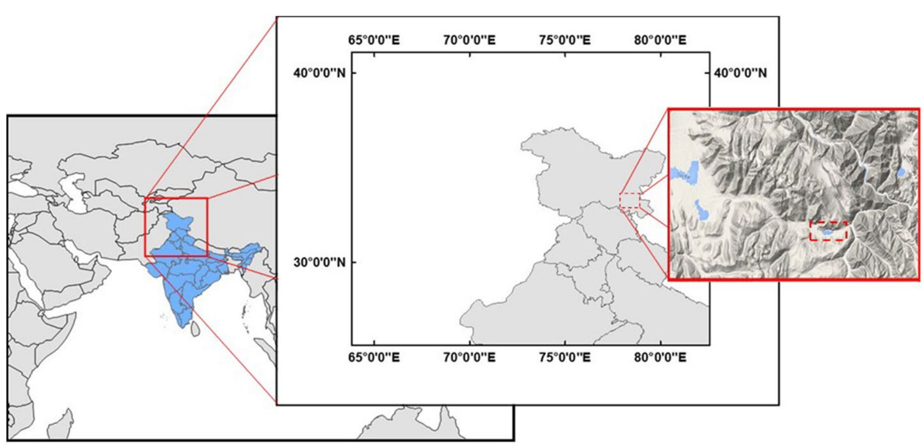

Fig. 1 Geographical location and terrain of Puga Valley, Ladakh, India

Valley is limited and also the exploration have been restricted to shallow depths (Geological Survey of India 1991).

Geophysical exploration of Puga geothermal valley

The Geological Survey of India initiated the geothermal investigation and usage on pilot arrangement scale in 1973 with the operation of Puga project in Jammu and Kashmir (Geological Survey of India 1991). A total of 34 discrete locations in the Puga geothermal manifestation zone have been selected for the borewell exploration. Well head measurements and the temperature logs are examined at seven borewell locations with depths ranging from minimum 28.5 m to maximum 384.7 m. The boreholes that harnessed shallow geothermal reservoir yielded steam of 10–15% quality at temperatures up to 140 °C and pressure ranging between 1.9 to 2.9 E5 Pa. Discharges of water and steam mixtures at temperatures of around 125 °C have been found from some of the boreholes at Puga for 15 years. The well-head measurements carried out at few of these borewell locations indicate a total discharge of 190 tonnes/h of water-steam mixture. In Fig. 2, PGW refers to Puga geothermal well and it is followed by a number. The deep geothermal reservoir is represented as PDGW (Puga deep geothermal well). The spatial location of PDGW is represented with a numerical value of "0" on the map shown in this study.

Gauged well data

Even though 34 locations have been identified for well exploration, the temperature vs. depth data and hydrogeological parameters are gauged and reported only at 7 locations named as PGW 20, PGW 18, PGW 6, PGW 15, PGW 3, PGW 1 and PDGW (Shanker et al. 1975). The status of the thermal gradient at ungauged well locations was not reported in the Geological Survey of India (1991). The temperature vs. depth data at only gauged locations as reported in Geothermal Atlas of India are shown in Fig. 3. These data are further used as the base data for regression analysis and finally providing the data for 2D Kriging.

Figure 3 shows that all the borewell locations have not been gauged to a unique depth. However, it can be noticed that temperature vs. depth data corresponding to seven locations are available to a common depth of 50 m. Hence, the study is restrained to provide 2D temperature distribution for thermal manifestation zone to the maximum depth of

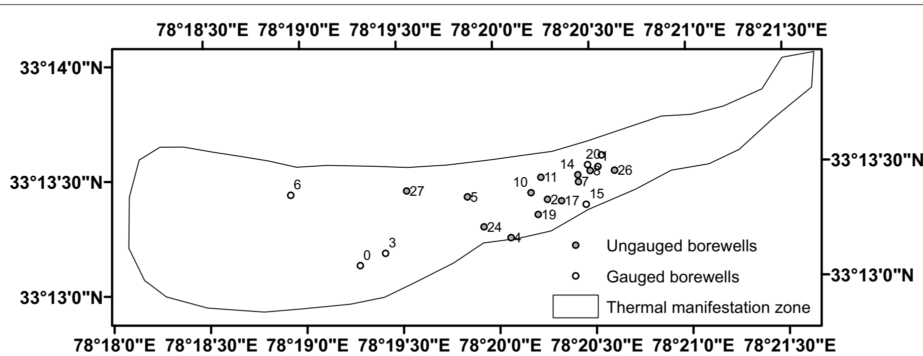

Fig. 2 Gauged and ungauged well locations of Puga geothermal manifestation zone

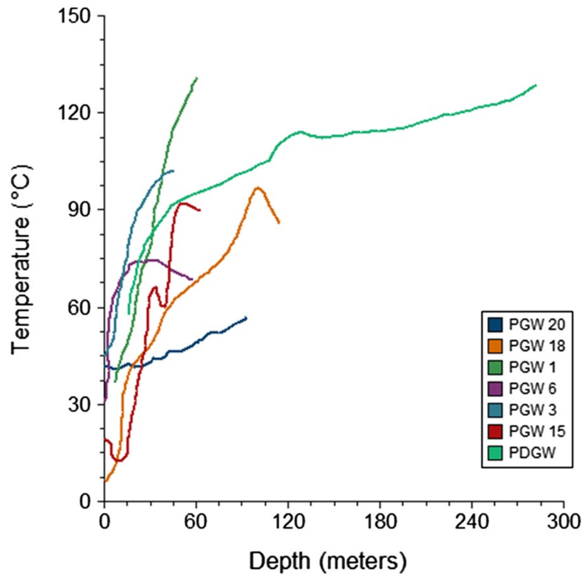

Fig. 3 Temperature vs. depth at gauged wells (Geological Survey of India 1991)

50 m by using Kriging interpolation. The approach adopted in this study can be used to evaluate 2D temperature distribution at greater depths provided that the temperature vs. depth data from the gauged locations is available due to deep exploration.

From Fig. 3, it is understandable that the temperature vs. depth data of PGW 1 and PDGW are not reported for the first few metres from surface (Geological Survey of India 1991). Furthermore, the physical exploration data of PGW 3 is not reported beyond 45 m. Therefore, ordinary least square (OLS) regression is used to capture the temperature vs. depth relation at each of the gauged borewell locations to 50 m from the surface. The regression equation developed for each of the gauged borewell location utilizes 85% of the data points available from Fig. 3 and rest of the 15% of data are used for the validation.

Temperature vs. depth relation by regression analysis

Temperature vs. depth relationships are established for seven gauged borewell locations. The Levenberg–Marquardt (LM) optimisation algorithm is used to evaluate all the standard functions. From the chosen best fit functions that accommodate the trend for temperature vs depth at these locations, it is observed that the coefficient of determination of these functions ranges from 0.86 to 0.98 as shown in Table 1. Seven trends fitting into the available data corresponding to seven gauged locations are shown in Table 1. The derived regression equation is used to evaluate temperature at 0, 10, 20, 30, 40 and 50 m of depth for each gauged well location. The regression equation also estimates temperature for unreported depths for PGW 1, PDGW and PGW 3.

Statistical validation with the field data

The mean percentage deviation between the field temperature data and the temperature data from regression relations is estimated by Eq. 3.

Table 1 Temperature vs. depth equations at gauged well locations by regression analysis

Well number	Distribution function *T*(*z*)	R^2
PGW 20	$40.24 + 0.11$ z	0.87
PGW 18	$6.99 + 1.46$ z	0.87
PGW 1	$19.53 + 2.08$ z	0.98
PGW 6	$\frac{a+bz}{1+cz+dz^2}$ $a = 24.26; b = 13.71; c = 0.121; d = 0.001$	0.94
PGW 3	$48.5 + 1.49$ z	0.89
PGW 15	$3.28 + 1.15$ z	0.86
PDGW	$45.69 + 1.14$ z	0.92
Natural geothermal gradient	$10.3 + 0.20$ z	0.98

Temperature field is in °C; *z* is the depth from surface in m

$$\text{Percentage of Deviation} = \left| \frac{\text{Observed } (T_\text{o}) - \text{Predicted } (T_\text{f})}{\text{Observed } (T_\text{o})} \times 100 \right|, \tag{3}$$

where T_o = Observed temperature at depth "d" as shown in Fig. 3, T_f = Predicted temperature at depth "d" using regression functions given in Table 2.

The mean absolute percentage deviation (MAPD) between the field temperature and estimated temperature is calculated for each borewell. The MAPD corresponding to PGW 20, PGW 18, PGW 1, PGW 6, PGW 3, PGW 15 and PDGW are 1.5, 13.9, 1.95, 3.49, 6.08, 8.52 and 8.27, respectively. The MAPD corresponding to PGW 18 and PGW 15 is relatively high as the trend is captured using a set of linear equations, whereas the observed trend is non-linear for these wells. However, a linear trend is observed in initial 50 m of depth for nearly all the wells. Therefore, the trend follows linear equations for all wells except PGW 6. Furthermore, it is also observed that the MAPD for each of the gauged wells is within 15%. Hence, the regression equations are adopted to generate the data required for Kriging to obtain 2D temperature distribution at specified depths.

Using regression equations, temperature at every 10 m of depth to 50 m is estimated for seven gauged well locations as shown in Table 2. The estimated data shown in Table 2 are used to project 2D temperature distribution for thermal manifestation zone at the specified depths by Kriging. The data from wells PGW 5 and PGW 10 are not used for Kriging. These wells which have been reported in Geological Survey of India SP3 (Shanker et al. 1981) are further used in validating the projected 2D temperature distribution.

Table 2 Temperature data at gauged locations using regression equations

Depth from surface (m)	Temperature at the gauged well locations in °C						
	PGW 20	PGW 18	PGW 1	PGW 6	PGW 3	PGW 15	PDGW
0	40.2	7.0	19.5	24.3	48.5	3.3	45.7
10	41.3	21.6	40.3	68.6	63.4	14.8	57.1
20	42.4	36.2	61.1	74.8	78.3	26.3	68.5
30	43.5	50.8	81.9	73.6	93.2	37.8	79.9
40	44.6	65.4	102.7	70.5	108.1	49.3	91.3
50	45.7	80.0	123.5	66.8	123.0	60.8	102.7

Kriging interpolation

Among the feasible geostatistical interpolation techniques, Kriging is an approximate method used widely in the field of geostatistics. A variogram measures the variance between pairs of points at a distance of "h" (lag distance) in terms of function in "h". Summation is taken over $m(h)$ pairs of points that are separated by a distance ranging between $h - d/2$ and $h + d/2$. A variogram is evaluated at various lag distances h separated by the variogram increment d. The functional relationship between the variance and the lag distance is computed mathematically by Eq. 4 (Webster and Oliver 2007).

$$\hat{\gamma}(h) = \frac{1}{2m(h)} \sum_{i=1}^{m(h)} \left\{ t(x_i) - t(x_i + h) \right\}^2, \tag{4}$$

where $\hat{\gamma}(h)$ is the variance, $t(x_i)$ is the observed field temperature value at the location x_i.

Geostatisticians have developed a number of model types to fit the full range of results obtained from variogram analyses. The most commonly used models are circular, spherical, pentaspherical, exponential and Gaussian (Gundogdu and Guney 2007). The anatomy of the circular, spherical, pentaspherical, exponential and Gaussian is well known from literature (Webster and Oliver 2007). The evaluated variogram using Eq. 4 is examined with reference to empirical variograms to choose the best fit mathematical model. The selection of the best fit model is followed by the execution of Kriging at the ungauged locations. The interpolated value of the temperature at the ungauged location is given by Eq. 5.

$$T(x) = \sum_{i=1}^{N} w_i t(x_i), \tag{5}$$

where $T(x) =$ Temperature at the ungauged location, $w_i =$ Weightage allotted to the sampled locations which is proportional to the variance between the target point and the neighbouring points, $t(x_i) =$ Observed field temperature at the gauged locations.

The temperature value at the ungauged locations is assessed by the weighted combinations of the neighbouring samples with respect to both distance and redundancy. The individual weights are assigned on the basis of minimizing the Kriging variance. This ensures the most precise estimates possible from the available data. The estimates are considered as good if the model fits to the observed variogram values. Thus, it is important that the variogram is accurate over the whole area of estimation. This method is widely used to determine the temperature at regional as well as local scale. From 2D temperature plots obtained by Kriging, the thermal gradients at all the ungauged well locations are estimated. Similarly, thermal gradients for new locations can also be obtained, if needed.

Results and discussion

In this study, ordinary Kriging is used to map temperature by using the field data from gauged well locations which is spread over an area of 3 km^2 representing the thermal manifestation zone of the Puga Valley. The temperature vs. depth data for gauged well locations as shown in Table 2 are used to generate variograms at specified depths.

Sample variograms at 0, 20 and 30 m depths are shown in Fig. 4. The estimated variograms at these depths conclude that the exponential model is the best fit model. Since the temperature vs. depth function is not unique for all the bore well locations, the same variogram may not fit for all the temperature distribution at considered depths. Keeping this fact into consideration, different variograms are provided at different depths.

2D temperature distribution for thermal manifestation zone at depths of 0, 10, 20, 30, 40 and 50 m is shown in Figs. 5, 6, 7, 8, 9 and 10, respectively. The isolines are shown at regular intervals of temperature. From 2D temperature plots, it is noted that the temperature as high as 50 °C is identified at surface level which indicates the existence of natural hot springs. From 2D temperature plots at various depths, it can also be noticed that the temperature change is steeper with depth. This is explicable from the denser isolines at greater depths.

From these 2D Kriging results, the temperature variations at ungauged locations are evaluated. The projected temperature vs. depth data at the ungauged locations are shown in Fig. 11. Figure 11 also shows that a temperature of 86 and 98 °C is achieved at the ungauged locations PGW 27 and PGW 26, respectively, within the depth of 50 m. The ungauged locations of PGW 7 and PGW 14 show least temperature of 67 and 63 °C, respectively, at 50 m depth. Also, average thermal gradients at all the gauged and ungauged

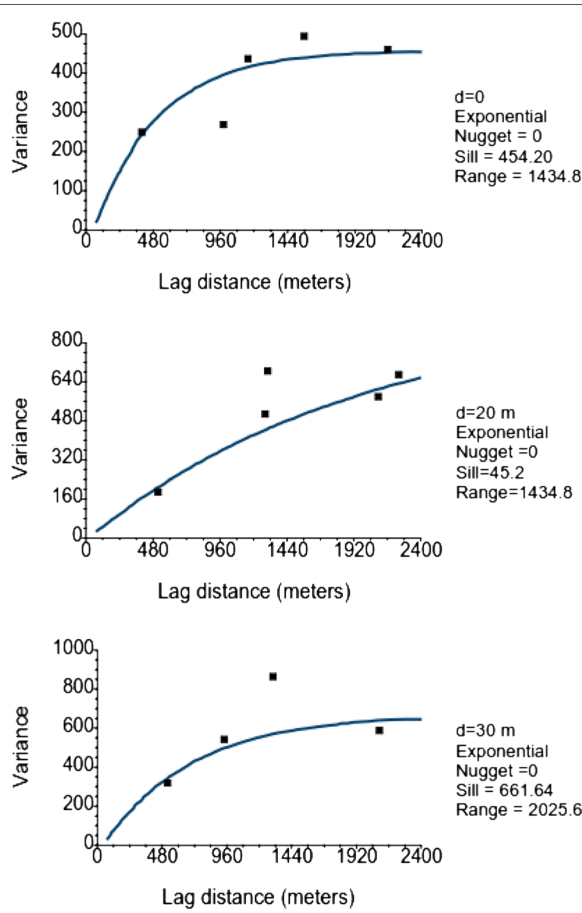

Fig. 4 Sample variograms of temperature data at 0, 20 and 30 m depths

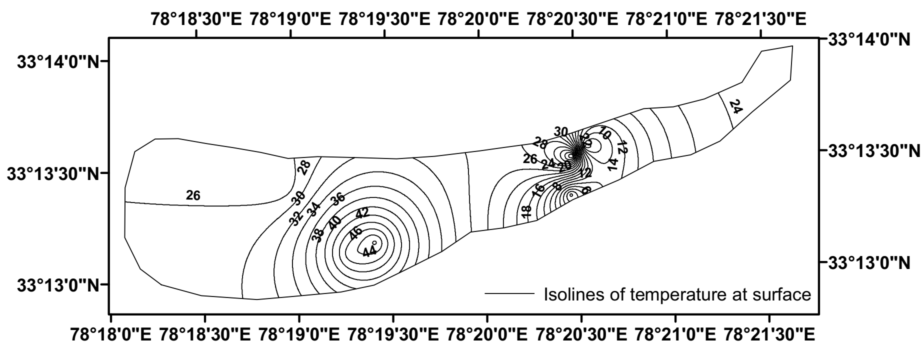

Fig. 5 Temperature contour for thermal manifestation zone at surface

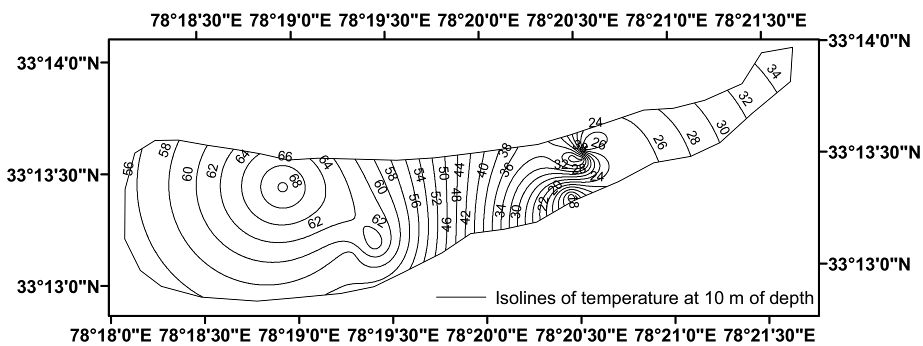

Fig. 6 Temperature contour for thermal manifestation zone at 10 m

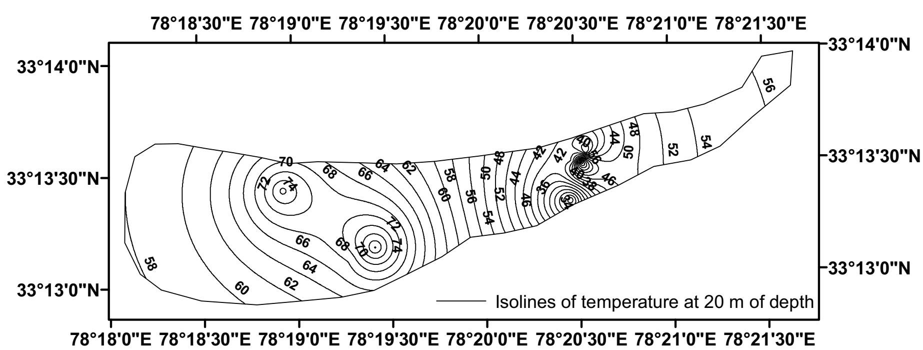

Fig. 7 Temperature contour for thermal manifestation zone at 20 m

locations are estimated to predict the priority order for the identified borewell locations. This priority order may help in making decisions for future explorations in terms of identifying the probable locations of injection and production wells in reservoir planning.

In Fig. 12a, the spatial distribution of gauged and ungauged well locations in the thermal manifestation zone is indicated. The histogram in Fig. 12b represents average thermal gradients at all gauged and ungauged locations sequentially located from west to east in the thermal manifestation zone of the Puga Valley. From Fig. 12b, it is observed that thermal gradient for some of the wells located towards the east of the valley is

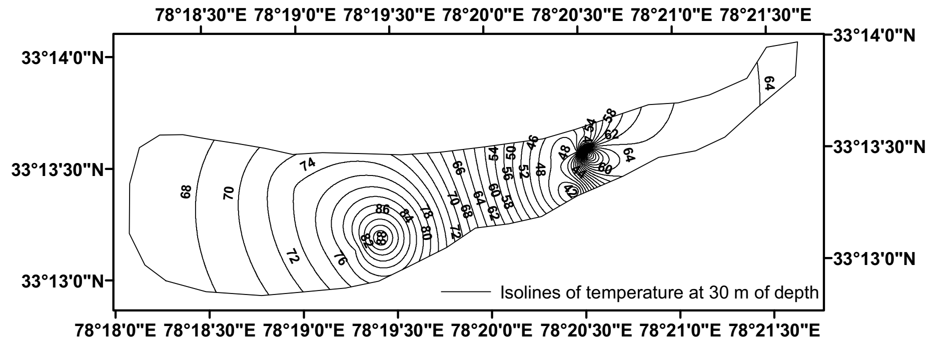

Fig. 8 Temperature contour for thermal manifestation zone at 30 m

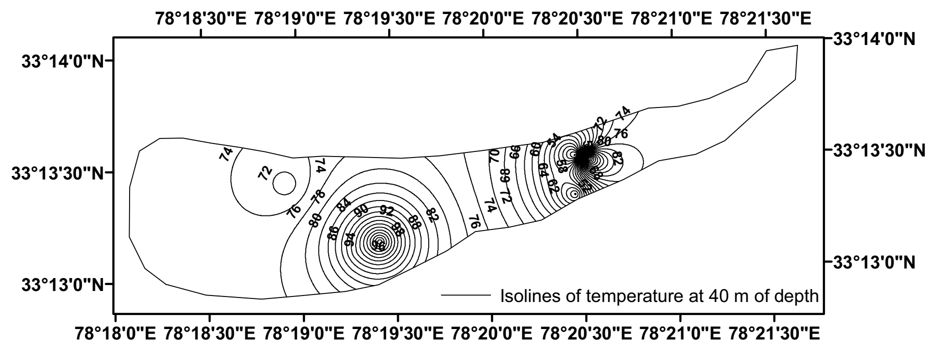

Fig. 9 Temperature contour for thermal manifestation zone at 40 m

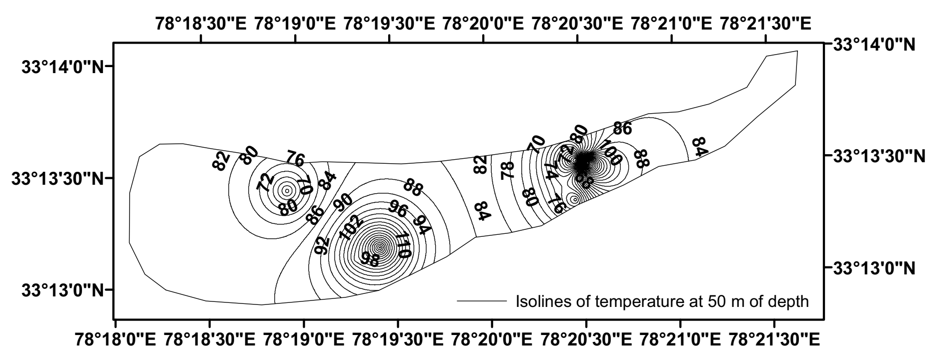

Fig. 10 Temperature contour for thermal manifestation zone at 50 m

relatively high. The observed high thermal gradients in eastern part of the valley satisfy the fact that a heat source is expected at the east of the valley at shallow depth (Azeez and Harinarayana 2007). Figure 12b shows that the thermal gradient of 1.7 °C/m at PGW 26 is highest among all the gauged and ungauged well locations. Based on the geographical distribution of well locations and their respective thermal gradients, the injection and extraction well comprising a system of doublet can be proposed and studied for energy extraction potential of the reservoir. The geothermal gradient at location of PGW 1 follows geothermal gradient at PGW 26 in the preferential order list.

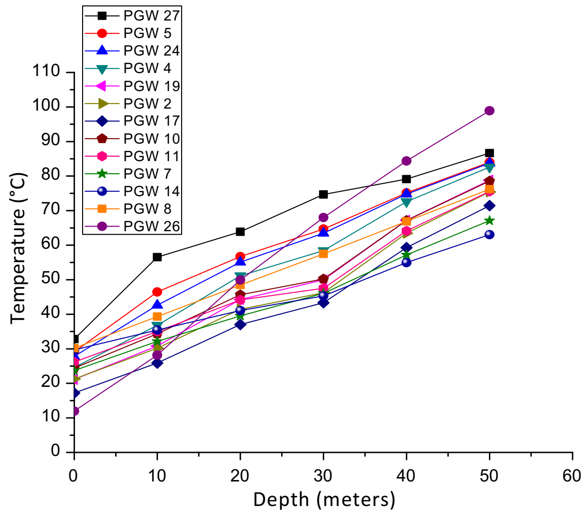

Fig. 11 Temperature vs. depth data at ungauged locations

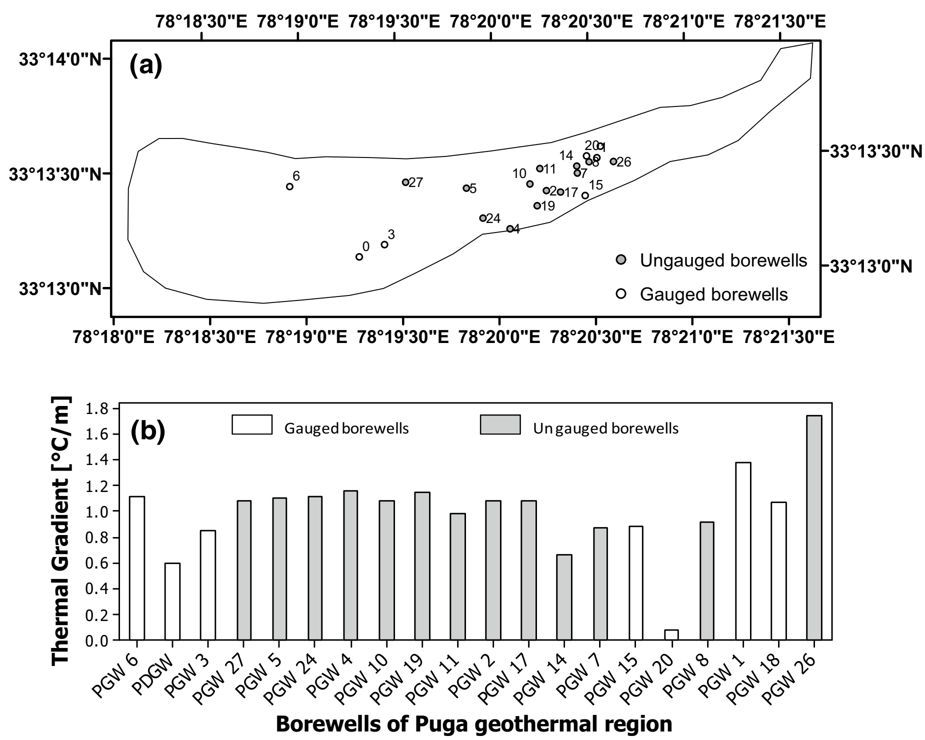

Fig. 12 **a** Gauged and ungauged locations. **b** Average thermal gradient at gauged and ungauged locations

The average thermal gradient of PGW 5 and PGW 10 obtained by Kriging is compared with the field data and it is observed that the deviation of Kriging result compared to the field result of PGW 5 is acceptable, whereas the results of PGW 10 is not agreeable. This condition is explicable by the fact that the zone under consideration is strongly influenced by heat convection leading to the heterogeneity as far as the shallow reservoir condition is concerned. Additionally, this deviation is possibly influenced by the heterogeneous rock setting.

The temperature distribution along a vertical cross section is shown in Fig. 13, which shows that the temperature initially increases followed by a decreasing trend while moving from west to east in the valley along the considered cross section. This trend is explicable by the fact that a heat source exists in the eastern part of the valley (Azeez and Harinarayana 2007). The trend may differ if another vertical cross section was considered in the manifestation zone. Such study of temperature distributions along vertical cross sections located in different directions may enable us to draw a generic trend of temperature distribution for the entire valley.

Conclusions

This study aims to predict 2D temperature distribution in thermal manifestation zone of the Puga Valley and thermal gradients at ungauged well locations. To attain this objective, Kriging technique is used to evaluate 2D temperature distribution for thermal manifestation zone at various depths. The variogram studies show that the exponential model is the best fit model for mapping the 2D temperature distribution in the Puga geothermal reservoir. It is also noticed that the thermal gradient at locations of PGW 26, PGW1, PGW 4 and PGW 19 is relatively high compared to rest of the locations. Finally, a priority order is drawn based on higher thermal gradient to lower thermal gradient by considering all gauged and ungauged locations (PGW 26 > PGW 1 > PGW 4 > PGW 19 > PGW 24 > PGW 6 > PGW 5 > PGW 17 > PGW 10 > PGW 2 > PGW 27 > PGW

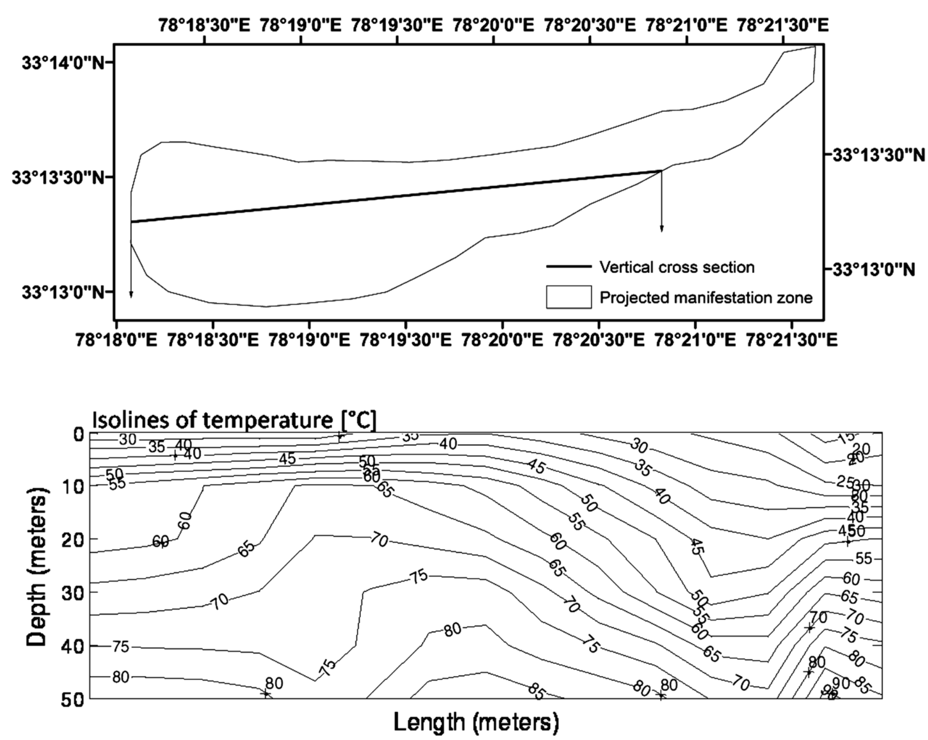

Fig. 13 Temperature contour along a specified vertical cross section

18 > PGW 11 > PGW 8 > PGW 15 > PGW 7 > PGW 3 > PGW 14 > PDGW > PGW 20). Also, thermal gradients at gauged and ungauged locations help in identifying the zones of high and low temperature. This may also be helpful in making the decisions for the future exploration of existing wells. The study of 2D mapping of temperature for greater depths is impaired due to the lack of deep reservoir data. However, the outcome of the study may be helpful in setting up the initial or equilibrium condition of the reservoir. Such equilibrium temperature distribution is needed for coupled fluid flow and energy transport simulations to estimate the energy withdrawal capacity of geothermal reservoir. This study may be extended to map 3D temperature distribution of the Puga geothermal reservoir, provided the explored data are well distributed in the valley.

Authors' contributions
The authors declare equal contribution towards the manuscript. Both authors edited the final manuscript. Both authors read and approved the final manuscript.

Acknowledgements
The authors acknowledge the host institute, Birla Institute of Technology and Science, Pilani, for supporting the present work under Doctoral Research Scheme.

Competing interests
The authors declare that they have no competing interests.

Availability of data and materials
All relevant data and material are presented in the main paper.

Publisher's Note
Springer Nature remains neutral with regard to jurisdictional claims in published maps and institutional affiliations.

Received: 24 July 2016 Accepted: 30 March 2017
Published online: 04 April 2017

References
Agemar T, Schellschmidt R, Schulz R. Subsurface temperature distribution in Germany. Geothermics. 2012;44:65–77. doi:10.1016/j.geothermics.2012.07.002.
Azeez KA, Harinarayana T. Magnetotelluric evidence of potential geothermal resource in Puga, Ladakh, NW Himalaya. Curr Sci. 2007;93(3):323.
Bishop TFA, Mc Bratney AB. A comparison of prediction methods for the creation of field-extent soil property maps. Geoderma. 2001;103(1):149–60. doi:10.1016/S0016-7061(01)00074-X.
Bonte D, Guillou-Frottier L, Garibaldi C, Bourgine B, Lopez S, Bouchot V, Lucazeau F. Subsurface temperature maps in French sedimentary basins: new data compilation and interpolation. Bull Soc Geol Fr. 2010;181(4):377–90. doi:10.2113/gssgfbull.181.4.377.
Chandrasekharam D, Chandrasekhar V. Geothermal energy resources, India: Country update, proceeding of world geothermal congress 2015. Melbourne, Australia; 2015.
Chiles JP, Gable R. Three-dimensional modelling of a geothermal field. Geostat Nat Resour Charact. 1984;2:587–98.
Craig J, Absar A, Bhat G, Cadel G, Hafiz M, Hakhoo N, Thusu B. Hot springs and the geothermal energy potential of Jammu & Kashmir State, NW Himalaya, India. Earth Sci Rev. 2013;126:156–77. doi:10.1016/j.earscirev.2013.05.004.
Garibaldi C, Guillou-Frottier L, Lardeaux JM, Bonte D, Lopez S, Bourgine B, Bouchot V. Relationship between thermal anomalies, geological structures and fluid flow: new evidences in application to the Provence basin (south-east France). Bulletin de la Societe Geologique de France. 2009.
Geological Survey of India. Geothermal atlas of India. In: Shanker R, editor. Geological Survey of India; 1991.
Guha SK. Status of exploration for geothermal resources in India. Geothermics. 1986;15(5):665–75.
Gundogdu KS, Guney I. Spatial analyses of groundwater levels using universal kriging. J Earth Syst Sci. 2007;116(1):49–55. doi:10.10007/s12040-007-0006-6.
Gupta ML. Geothermal energy: a secure resource for development of Ladakh Region, India, GRC transactions. 2009; 33.
Harinarayana T, Azeez KA, Murthy DN, Veeraswamy K, Rao SE, Manoj C, Naganjaneyulu K. Exploration of geothermal structure in Puga geothermal field, Ladakh Himalayas, India by magnetotelluric studies. J Appl Geophys. 2006;58(4):280–95. doi:10.1016/j.jappgeo.2005.05.005.
Kruger P. Heat extraction from HDR geothermal reservoirs. In Proceeding World Geothermal Congress ; 1995. p. 2517–20.
Li J. A review of spatial interpolation methods for environmental scientists. 2008.
Moyeed RA, Papritz A. An empirical comparison of Kriging methods for nonlinear spatial point prediction. Math Geol. 2002;34(4):365–86.

Rühaak W. 3-D interpolation of subsurface temperature data with measurement error using kriging. Environ Earth Sci. 2014;73(4):1893–900. doi:10.1007/s12665-014-3554-5.
Rühaak W, Bar K, Sass I. Combining numerical modelling with geostatistical interpolation for an improved reservoir exploration. Energy Proced. 2014;59:315–22. doi:10.1016/j.egypro.2014.10.383.
Shanker R, Padhi RN, Arora CL, Prakash G, Thussu JL, Dua KJS. Geothermal exploration of the Puga and Chumathang geothermal fields, Ladakh, India. In Proceedings, Second United Nations Symposium on the Development and Use of Geothermal Resources, San Francisco, USA; 1975. p. 20–9.
Shanker R, Padhi RN, Arora CL, Prakash G, Thussu JL, Dua KJ. Geothermal exploration of the Puga and Chumathang geothermal fields, Ladakh, India. Geological survey of India-3, Lucknow, Uttar Pradesh, India; 1981.
Shanker Ravi, Padhi RN, Prakash G, Thussu JL, Wangdus C. Recent geological studies in upper Indus valley and the plate tectonics. Geol Surv India Misc Publ. 1976;34:41–56.
Tewari AP. On the upper Tertiary deposits of Ladakh Himalayas and correlation of various geotectonic units of Ladakh with those of the Kumaon-Tibet region. In Proceeding international geological congress 22nd session, New Delhi, 11; 1964. p. 37–58.
Verfaillie E, Van Lancker V, Van Meirvenne M. Multivariate geostatistics for the predictive modelling of the surficial sand distribution in shelf seas. Cont Shelf Res. 2006;26(19):2454–68.
Webster R, Oliver MA. Geostatistics for environmental scientists. Amsterdam: Wiley; 2007.